Atmos. Meas. Tech. Discuss., https://doi.org/10.5194/amt-2017-439
Manuscript under review for journal Atmos. Meas. Tech.
Discussion started: 7 December 2017

Atmospheric Measurement Techniques Discussions

Title: X-BAND DUAL-POLARIZED RADAR QUANTITATIVE PRECIPITATION ESTIMATE ANALYSES IN THE MIDWESTERN UNITED STATES

Authors: Micheal J. Simpson[1] and Neil I. Fox[2]

Micheal J. Simpson[1*]

Cooperative Institute of Mesoscale Meteorological Studies, University of Oklahoma.

National Severe Storms Laboratory, Norman, Oklahoma.

Tel: +001 4053256459

Email: micheal.simpson@noaa.gov

Neil I. Fox[2]

University of Missouri, School of Natural Resources, Water Resources Program, Department of Soil, Environmental, and Atmospheric Sciences, 332 ABNR Building, Columbia, Missouri, USA, 65201.

Tel: +001 5738822144

Email: FoxN@Missouri.edu

***Corresponding Author**: Micheal J. Simpson (mjs5h7@mail.missouri.edu)

Abstract. Over the past decade, polarized weather radars have been at the forefront of the search for a replacement of estimating precipitation over the spatially, and temporally inferior tipping buckets. However, many radar-coverage gaps exist within the Continental US (CONUS), proposing a dilemma in that radar rainfall estimate quality degrades with range. One possible solution is that of X-band weather radars. However, the literature as to their long-term performance is lacking. Therefore, the overarching objective of the current study was to analyze two year's worth of radar data from the X-band dual-polarimetric MZZU radar in central Missouri at four separate ranges from the radar, utilizing tipping-buckets as ground-truth precipitation data. The conventional R(Z)-Convective equation, in addition to several other polarized algorithms, consisting of some combinations of reflectivity (Z), differential reflectivity (ZDR), and the specific differential phase shift (KDP) were used to estimate rainfall. Results indicated that the performance of the algorithms containing ZDR were superior in terms of the normalized standard error (NSE), missed and false precipitation amounts, and the overall precipitation errors.

Furthermore, the R(Z,ZDR) and R(ZDR,KDP) algorithms were the only ones which reported NSE values below 100%, whereas R(Z) and R(KDP) equations resulted in false precipitation amounts equal to or greater than 65% of the total gauge recorded rainfall amounts. The results show promise in the utilization of the smaller, more cost-effective X-band radars in terms of quantitative precipitation estimation at ranges from 30 to 80 km from the radar.

Introduction

Since the late 20th Century, weather radars have been at the forefront of multiple studies to determine their accuracy in determining precipitation estimation (e.g., Kitchen and Jackson, 1993; Smith et al., 1996; Ryzhkov et al., 2003; Cunha et al., 2013; Simpson et al., 2016). Multiple researchers have reported accurate measurements in radar rainfall estimates when compared to terrestrial-based precipitation gauges (e.g., tipping buckets). This has several important implications for multi-disciplinary fields which rely on highly spatialized and temporal precipitation data, which can be obtained from radar estimates compared to the spatially inferior rain gauges.

Most studies in the US have utilized the National Weather Service (NWS) Next Generation Radar (NEXRAD) system, comprised of Weather Surveillance Radar – 1988 Doppler (WSR-88D) series instruments, operating at S-band (approximately, 10 – 11 cm) wavelength for their analyses. However, the cost of installation and maintenance of these instruments are much larger in comparison to the smaller, lighter-weighted X-band radars, operating at, approximately, 3 cm wavelength (Matrosov 2010). Berne and Krajewski (2013) have stated that, primarily due to the sparse coverage of the WSR-88D S-band radar system, smaller, more frequently-placed X-band radars are a viable option for remediating radar rainfall errors that have been recorded at large distances (e.g., Smith et al., 1996; Ryzhkov et al., 2005; Simpson et al., 2016). Although long-term NWS studies have been conducted (Haylock et al., 2008;

Atmos. Meas. Tech. Discuss., https://doi.org/10.5194/amt-2017-439
Manuscript under review for journal Atmos. Meas. Tech.
Discussion started: 7 December 2017

Fairman et al., 2012; Goudenhoofdt and Delobbe 2012, 2016), the literature of multi-year studies of X-band weather radars is not as abundant.

Matrosov et al. (2002) conducted a study analyzing 15 separate rainfall events during an eight-week field campaign in Virginia while utilizing the National Oceanic and Atmospheric Administration's (NOAA) X-band dual-polarimetric radar. Several radar rainfall algorithms were implemented, including combinations of the equivalent reflectivity (Z_e), differential reflectivity (ZDR), and the specific differential phase-shift (KDP), an R(KDP) equation, and two R(Z_e) relations, over a region with three ground-truthed rain gauges. It was found that the combined polarimetric estimator (i.e., utilization of Z_e, KDP, and ZDR) resulted in the overall least standard deviation (22%), while the case-tuned R(Z_e) relation was slightly higher of 23%. It is noted that R(Z_e) measurements are derived from a priori knowledge of Z_e, KDP, and ZDR values, whereas the combined polarimetric estimator was not, implying the latter is superior for real-time use. However, the performance of the combined polarimetric estimator works best when rain rates exceeded 1.5 mm h^{-1}, while R(Z_e) algorithms were superior at lighter rain rates. Results from the R(KDP) algorithm reported an overall negative bias of 6-9% when compared to the gauge data, in addition to a standard deviation of 30%, primarily due to the sensitivity of KDP measurements while utilizing X-band radars.

Expanding upon the literature of implemented R(KDP) algorithms through X-band radars, Wang and Chandrasekar (2010) assessed the performance of three separate R(KDP) algorithms from the Collaborative Adaptive Sensing of the Atmosphere (CASA) Engineering Research Center through the use of the distributed collaborative adaptive sensing (DCAS) network. The DCAS network, essentially, implements multiple radar networks within a relatively small spatial extent, all operating at different volume coverage patterns (VCP's) such that high spatiotemporal resolution data is achieved in addition to overall lower beam height over the area of interest (McLaughlin et al., 2009), mitigating effects that have been observed due to rain rate estimations at large ranges (Kitchen and Jackson, 1993; Ryzhkov et al., 2005; Simpson et al., 2016). The results indicated that through the use of several different R(KDP)

Atmos. Meas. Tech. Discuss., https://doi.org/10.5194/amt-2017-439
Manuscript under review for journal Atmos. Meas. Tech.
Discussion started: 7 December 2017

Atmospheric Measurement Techniques Discussions

algorithms from multiple different radars, radar Quantitative Precipitation Estimates (QPE) can be improved significantly. Furthermore, the R(KDP) algorithms exhibited similar bias values (between -6 and 8 %) that were reported by Matrosov (2002) and Matrosov et al. (2010). However, the normalized standard error (NSE) values ranged from, approximately, 16 to 54%, indicating that the overall error in R(KDP) rain rate estimates were less than half of the total amount of rain observed for the study.

The overarching objective of the current study is to add to the relatively few articles on X-band dual-polarization radar rain rate performance. Authors have proposed (e.g., Berne and Krajewski 2013) that the capability of implementing more X-band radars in comparison to the relatively sparse and expensive S-band WSR-88D NEXRAD system to enhance precipitation estimation is a viable option (particularly over the inter-mountain West), especially for hydrologic analyses. However, others (e.g., McLaughlin et al., 2009) suggest the sheer number of radars to achieve such a difference in radar rain rate estimation is impractical. Further justification for increasing, at least partially, the construction of X-band weather radars is necessary through analyses of those that already exist.

The current study analyzes two year's of radar data from the newly-installed dual-polarimetric MZZU X-band radar located in Central Missouri. Over 100 different algorithms were implemented to test the performance of the radar while utilizing measurements of reflectivity (Z), differential reflectivity (ZDR), and the specific differential phase shift (KDP). Rain rates were calculated based on combinations of the aforementioned variables and compared to four separate tipping buckets, which served as ground-truth. To determine the performance of all algorithms, multiple statistical analyses were conducted, including the bias, mean absolute error, and normalized standard error. Additionally, several contingency factors were calculated, such as the overall number of hits, misses, false alarms, and correct negatives. Lastly, quantitative analyses, including the missed precipitation amount (MPA), false precipitation amount (FPA), and overall error were computed to determine the performance of the 108 algorithms. Analyses, such as the current study, are important for determining the accuracy and limitations of dual-polarimetric radars such that their incorporation into hydrologic models may be correctly assessed (Ogden

Atmos. Meas. Tech. Discuss., https://doi.org/10.5194/amt-2017-439
Manuscript under review for journal Atmos. Meas. Tech.
Discussion started: 7 December 2017

Atmospheric Measurement Techniques Discussions

et al., 1997; Vieux, 2004; Vieux et al., 2004; Vieux and Bedient, 2004; Gourley et al., 2010; Cunha et al., 2015). Furthermore, studies analyzing the performance of X-band radars will allow further indications as to whether they should be installed in regions devoid of optimal NWS WSR-88D coverage.

Data and methodology

Study location and gauge data

The dates analyzed ranged from August 2015 to August 2017 which, when accounting for radar down time for maintenance and offline issues, yielded 608 days, or 14952 hours for analyses. The current study was conducted in Boone County, located in Central Missouri (Figure 1), where the MZZU radar is located at 38.906°N and 92.269°W. Several Missouri Mesonet rain gauges lie within the domain of the MZZU radar, located in Versailles, Auxvasse, Williamsburg, and Vandalia, MO, located at, approximately, 75-km, 30-km, 45-km, and 80-km from the radar, respectively.

Missouri is characterized as a continental type of climate, marked by relatively strong seasonality. Furthermore, Missouri is subject to frequent changes in temperature, primarily due to its inland location and its lack of proximity to any large lakes. All of Missouri experiences below-freezing temperatures on a yearly-basis. The TE525 tipping bucket series performs optimally in temperature conditions between 0 and 50°C. Albeit no events recorded a daily maximum temperature above 50°C, 72 days in the cool season (e.g., January and February) recorded temperatures below 0°C. However, only 8 days that exhibited sub-freezing average daily temperatures registered precipitation. Thus, less than 1% of the entire data might be further unrepresentative of the actual precipitation. For this study, it was assumed since the amount of precipitation recorded by the gauges during these events were below 5 mm in precipitation, no significant errors would affect the overall statistics.

One tip from the fulcrum device registers 0.254 mm of precipitation, which is the minimum resolution required for statistics to be analyzed between the radar and the tipping gauge. In spite of the

Atmos. Meas. Tech. Discuss., https://doi.org/10.5194/amt-2017-439
Manuscript under review for journal Atmos. Meas. Tech.
Discussion started: 7 December 2017

well-documented literature discussing the errors associated with tipping buckets (e.g., Ciach and Krajewski, 1999a, 1999b; Habib and Krajewski 1999; Habib et al., 2001; Ciach 2002), the gauges are well-maintained and well-documented in terms of instrumentation failure, clogging, or other discrepancies with the devices. Therefore, they are assumed to be valid as ground-truth devices.

Radar discussion and data

The radar for the current study is part of the Missouri Experimental Project to Stimulate Competitive Research (EPSCoR) program, primarily aimed at enhancing Missouri's modelling capacity of weather and climate on plants and communities at the local, and regional scale. The X-band radar (MZZU) was installed in the Summer of 2015, in which data acquisition became possible by the Fall of 2015 near the South Farm Research Center, located in central Boone County, MO (Figure 1). The instrument is utilized, primarily, for research purposes, but is also quasi-operational. Specifics regarding the radar are detailed in Table 1.

Raw radar data were analyzed using the Weather Decision Support System – Integrated Information (WDSS-II) program (Lakshmanan et al., 2007a) to assess reflectivity (Z) in addition to dual-polarized radar variables including differential reflectivity (ZDR) and specific differential phase shift (KDP). Many different quality control techniques (e.g., Lakshmanan et al., 2007b, 2010, 2014) were implemented to the weather radar data processing with WDSS-II. Three other variables were also generated based on a KDP-based smoothing field (Ryzhkov et al., 2003) for reflectivity, differential reflectivity, and specific differential phase: DSMZ, DZDR, and DKDP, respectively. These were analyzed to determine whether the additional KDP-smoothing fields tend to over- or underestimate QPE's (Simpson et al., 2016).

All six variables (Z, ZDR, KDP, DSMZ, DZDR, and DKDP) were converted from their native polar grid to 256 x 256 1 km Cartesian grids, where the lowest radar elevation scans (0.5°) were used to mitigate uncalculated effects from evaporation and wind drift. An average of 5-minute scans were used for each of the variables, which were aggregated to hourly totals to be compared to the hourly tipping-bucket accumulations. In spite of previous reports suggesting 5 minute to hourly aggregates can have significant effects on QPE (Fabry et al., 1994), evidence has been presented that overestimation in accumulations may not exceed 26% for a pixel size of 1 km (Shucksmith et al., 2011).

The latitude and longitude of each of the 15 gauges were matched with the radar pixel that corresponds to the Cartesian grid value of the seven radar variables which were then implemented in rain rate calculations. Three single-polarized R(Z) algorithms were tested, including R(Z)-Convective, R(Z)-Stratiform, and R(Z)-Tropical. The dual-polarized algorithms implemented are based from previous S- and X-band research to more closely resemble the sensitivity of the radars on KDP estimates. Although, theoretically, the relationship between R and Z for a well calibrated radar as controlled by the drop size distribution should be independent of radar wavelength. However, as the phase shift of the wave is a function of the ratio of wavelength to drop radius, the R(KDP) relationships are wavelength dependent.

The five R(Z,ZDR) S-band equations tested by Simpson et al. (2016) were implemented, whereas six, three, and two X-band R(KDP) algorithms were adopted from Matrosov (2010), Wang and Chandrasekar (2010), and Koffi et al. (2014) (Table 2). Additionally, two X-band R(Z,ZDR) and R(ZDR,KDP) algorithms were adopted from Matrosov (2010) and Koffi et al. (2014), respectively. All measures of Z, ZDR, and KDP were tested in addition to their KDP-smoothed derivatives, DSMZ, DZDR, and DKDP. A rain rate echo classification variable (RREC) was also computed, which chooses whether an R(Z), R(KDP), R(Z,ZDR), or R(ZDR, KDP) algorithm is implemented in estimating rain rates based on the radar fields of Z, ZDR, and KDP (Kessinger et al., 2003). This echo classifier will provide evidence as to whether a multi-parameter algorithm is superior to the single algorithms.

Furthermore, algorithms were grouped based on the variables implemented to estimate rain rates. Collectively, three R(Z) algorithms were tested, R(Z)-Convective, R(Z)-Stratiform, and R(Z)-Tropical, in addition to the DSMZ counterparts. Five separate R(Z,ZDR) equations were also implemented, including

Atmos. Meas. Tech. Discuss., https://doi.org/10.5194/amt-2017-439
Manuscript under review for journal Atmos. Meas. Tech.
Discussion started: 7 December 2017

five R(Z,DZDR), five R(DSMZ,ZDR), and the five R(DSMZ,DZDR) combinations. These 26 equations encompass the S-band algorithms to be tested on the X-band radar, to determine how versatile the equations are. Conversely, there were eleven R(KDP) X-band algorithms (and, thus, eleven R(DKDP) equations), two R(Z,ZDR), and two R(ZDR,KDP) equations in addition to their DSMZ, DZDR, and DKDP variables.

Statistical, contingency, and quantitative analyses

The results were split between three different categories: statistical, contingency, and quantitative. The three statistics utilized included the bias, mean absolute error (MAE), and normalized standard error (NSE). The NSE was chosen in place of the root-mean-square-error (RMSE) due to the ambiguity of the measure (Willmott and Matsuura, 2005; Jerez et al., 2013). Contingency analyses included the number of hits, misses, and false alarms. Accounting for the quantitative measure of precipitation due to the number of misses and false alarms, the missed precipitation amount (MPA) and false precipitation amount (FPA) were calculated. Additionally, the sum of precipitation is presented to render a long-term performance (i.e., two year's) of the radar in comparison to the ground-truthed gauges.

Results and discussion

From the four separate gauges, Auxvasse was the closest to the radar (approximately, 30 km) while Vandalia was the furthest (80 km), with Versailles slightly closer at 75 km (Figure 1). Williamsburg lies 45 km from the radar, placing it near the middle of the group of gauges in terms of distance. The overall average amount of gauge recorded precipitation between the four sites was, approximately, 1650 mm (Figure 2). Excluding the warm season (approximately from April – September), the amount of gauge-recorded rainfall was similar across the four gauges. The large variance in precipitation during the warm season were due, primarily, from several isolated convective cells which were recorded at the certain gauges (e.g., Williamsburg), but missed at others (e.g., Versailles). The normalized standard error (NSE) was chosen as the statistic to assess the overall performance of each algorithm due to the (typical) non-Gaussian representation of precipitation (Kleiber et al., 2012; Alaya et al., 2017).

-

Smoothed versus non-smoothed QPE

For the 26 S-band equations analyzed, the R(Z)-Convective had the lowest NSE at Auxvasse (1.6), Williamsburg (1.51), and Versailles (1.59) whereas the R(Z)-Stratiform outperformed at the furthest gauge, Vandalia (1.64) (Figure 3). A pattern of the R(DSMZ)-Tropical and then R(Z)-Tropical performing the worst was exhibited, with the RREC performing worse than either the R(Z)- or R(DSMZ)-Convective and Stratiform equations. Although there were no significant ($p < 0.10$) differences between R(Z) and R(DSMZ), the difference between R(Z)-Tropical and R(DSMZ)-Tropical was significant ($p < 0.10$). These R(Z) algorithms in addition to the RREC performed best at 75 km from the radar, whereas 5 km further (Vandalia) displayed the largest NSE values. This may be due, at least in part, to the fact that single gauges were utilized as ground truth, whereby any of the numerous errors associated with tipping bucket rain gauges (Ciach and Krajewski 1999a; Habib et al. 2001; Ciach 2002) occurred.

Due to the small impact of smoothing the ZDR field (i.e., DZDR) on QPE, neither the R(Z,DZDR) nor R(DSMZ,DZDR) are reported. The addition of the DSMZ field was inferior for all R(Z,ZDR) equations in terms of NSE. Two National Severe Storm Laboratory (NSSL) derived R(Z,ZDR) equations (Ryzhkov et al., 2003) were superior compared to their R(DSMZ,ZDR) counter-parts. The R(Z,ZDR) and R(DSMZ,ZDR) equation 2 recorded the largest NSE values (neither recording values less than 2.5) since the equation was derived from a sub-tropical environment (Brandes et al., 2002). The NSE values for the single- and dual-pol equations ranged from 1.6 to 2.5 and 1.6 to 4.3 at a distance of 30 km from the radar, respectively. The range in NSE values were least for the gauge at 75 km from MZZU (less than 1.5 units).

Only the R(Z,ZDR)2 and R(DSMZ,ZDR)2 equations displayed a significant ($p < 0.10$) at each of the four gauges, demonstrating the significant impact smoothed reflectivity has on QPE. The other significant difference in QPE was at the closest gauge between R(Z,ZDR)1 and R(DSMZ,ZDR)1. These two algorithms were not derived by NSSL and, typically, performed the worst overall as the climatology of precipitation in which these equations were derived (Bringi and Chandrasekar, 2001; Brandes et al., 2002) were more tropical compared to the continental properties at the NSSL.

Statistical analyses

From the 68 algorithms overall, the best R(Z) equation was R(Z)-Convective, similar to the findings of Simpson et al. (2016). However, R(Z,ZDR)4 outperformed R(Z,ZDR)5, which displayed the lowest NSE in Simpson et al. (2016). Furthermore, the best R(KDP) algorithm was from Matrosov (2010), while the best performing R(ZDR,KDP) equation was from Koffi et al., (2014), algorithms 6 and 11 from Table 2, respectively. These were chosen to be the best overall algorithms from each grouping of equations due to their lowest MAE and NSE values (Table 3).

With Auxvasse being the closest gauge to the radar (30 km), this location registered the least bias across all grouping of algorithms, excluding RREC. In fact, the R(Z,ZDR) equation showed no bias (0.0 mm), while R(KDP), R(ZDR,KDP), and RREC displayed slightly positive biases (0.3, 0.3, and 0.5 mm, respectively). This is surprising since ZDR has not been calibrated for the MZZU radar, which has been shown to significantly alter QPE (Hubbert and Bringi, 1995; Atlas, 2002; Illingworth, 2004; Williams et al., 2005; Zrnic et al., 2010; Ice et al., 2013). Only the R(Z) equation registered a negative bias (-0.1 mm), consistent with the fact that the conventional R(Z) algorithm is inappropriate for stratiform precipitation (Klazura and Kelly, 1995; Seo et al., 2015). Interestingly, the RREC registered less bias as distance from the radar increased (0.5, 0.2, 0.2, and 0.1 mm for distances of 30, 45, 75, and 80 km, respectively) whereas most other algorithms displayed an increase in magnitude as the distance from MZZU increased.

Atmospheric Measurement Techniques Discussions

In general, Williamsburg, the second-furthest gauge from MZZU (45 km), registered the second-best bias with the notable exception of the R(Z) equation. For example, underestimation on the order of -0.3 mm was recorded at Williamsburg for R(Z), while -0.2 mm and -0.4 mm were registered at Versailles (75 km) and Vandalia 80 km), accordingly. Furthermore, Auxvasse was the only of the four gauges which did not register a negative bias for R(Z,ZDR). The largest biases were recorded by R(KDP).

The mean absolute errors values recorded by the R(Z,ZDR) equation were 1.3, 1.4, 1.4, and 1.5 mm at distances of 30, 45, 75, and 80 km, respectively. Otherwise, the other four algorithms represented increasing error with increasing range from MZZU, with the lowest MAE being R(ZDR,KDP) with 1.2 mm, and the largest being RREC (1.7 mm). This indicates that the RREC algorithms was incapable in correctly determining the proper QPE algorithm based on the values of radar variables and near storm environment surroundings.

At no locations for R(Z), R(KDP), or RREC did the normalized standard error fall below 100%. Therefore, the two algorithms containing the differential reflectivity recorded NSE's less than 100%, in particular at the two closest gauge locations. The R(ZDR,KDP) registered 84.7 and 93.1% at Auxvasse and Williamsburg, whereas R(Z,ZDR) displayed NSE values of 89.2 and 99.0%, respectively. Furthermore, these two algorithms calculated less NSE at the furthest location (Vandalia) than at the third furthest location (Versailles), in spite of there being a 5 km difference in range between the two locations, further demonstrating the impact of gauge errors on QPE (Sevruk, 2005; Rasmussen et al., 2012).

Contingency analyses

To determine where the bulk of errors implicit within the bias, mean absolute error, and normalized standard error originate from, contingency analyses were calculated, including hits, misses, and false alarms.

The number of tips recorded at Auxvasse, Vandalia, Versailles, and Williamsburg were 810, 725, 762, and 855, accordingly (Figure 5). In terms of the number of hits, misses, and false alarms, an analysis of variance (ANOVA) table was constructed to determine whether any significant differences exist between the five algorithms. Results indicate that, with 99% confidence, the number of hits between the five algorithms, in addition to the number of misses and false alarms did not differ significantly from one algorithm to the next. Therefore, the results of contingency analyses will be conducted utilizing the R(ZDR,KDP) algorithm to reduce redundancies.

The number of hits were 688, 603, 647, and 736 at Auxvasse, Vandalia, Versailles, and Williamsburg, respectively, indicating that 85, 83, 85, and 86% of the precipitation events were correctly assessed by the radar. With 122, 122, 115, and 119 misses, only 15, 17, 15, and 14% of rainfall events were missed. However, the occurrences of false alarms were similar to the number of hits and, for Vandalia, exceeded the number of gauge tips. For example, Auxvasse, Williamsburg, Versailles, and Vandalia registered 7 more, 4 more, 9 less, and 135 more false alarms than the number of hits. Therefore, it may be concluded that the bulk of the errors in the QPE's were, primarily, due to false alarms.

In spite of the prevalent occurrences of the number of false alarms, the correlation coefficient values between the gauge recorded and radar estimated precipitation were as large as 0.70, particularly for the R(Z)-Convective and RREC algorithms (Figure 6). Furthermore, these two algorithms had the same R^2 values for all of the four stations of 0.7, 0.68, 0.56, and 0.5 for Auxvasse, Williamsburg, Versailles, and Vandalia, respectively. The R(KDP) equation had similar values with the exception of Auxvasse, which was 0.69 (0.01 less).

The ZDR-containing algorithms have been shown to be superior to the other three equations in terms of NSE (Table 3), yet produced the, overall, lowest R^2 values. Therefore, the added benefit of dual-polarized parameters may be limited to certain types of hydrometeors (Cunha et al., 2015). The best values were 0.63 and 0.62 at Auxvasse for R(Z,ZDR) and R(ZDR,KDP), respectively, while the lowest values were 0.43 and 0.41 at Vandalia, accordingly. The reason for the findings may be due to the fact that the R(Z,ZDR) and R(ZDR,KDP) algorithms showed more spread in the correlation data, particularly at Auxvasse. Although the RREC displayed spread in the data as well, the magnitudes of error were,

Atmos. Meas. Tech. Discuss., https://doi.org/10.5194/amt-2017-439
Manuscript under review for journal Atmos. Meas. Tech.
Discussion started: 7 December 2017

Atmospheric Measurement Techniques Discussions

typically, contained below 15 mm as estimated by the radar. Furthermore, the radar tended to underestimate precipitation for R(Z) and RREC, but showed larger radar estimated precipitation for R(KDP) and R(ZDR,KDP), correlating with the bias values described earlier (Table 3).

Quantitative analyses

The quantitative analyses are the amount of precipitation associated with each miss, false alarm, or due to error overall. Additionally, the overall accumulation of precipitation over the course of the study is presented to determine whether the errors cancel out over longer time periods.

Although it was found that 15, 17, 15, and 14% of rainfall events were missed, this accounted for 6.5, 5.6, 11.0, and 11.6% of the error relative to the gauge for the R(Z)-Convective equation (Table 4). This indicates that, on average, most of the missed precipitation events were for values less than 1.0 mm. This may be due, at least in part, to the fact that tipping buckets are incapable of measuring the beginning of a precipitation event, or, very light rainfall periods (Ciach, 2002). For algorithms that did not contain ZDR, the furthest location (Vandalia) typically registered the largest MPA values, in addition to contributing the most amount of MPA compared to the gauge accumulated total for any of the four locations. The largest MPA for R(Z) was at Vandalia (180.8 mm), which was 11.6 of the total gauge amount, where QPE's estimated at Williamsburg only recorded 99.4 mm of MPA (5.6% of total). Although Williamsburg (second-furthest gauge) recorded the least amount of MPA for R(Z), R(KDP) and RREC, the closest gauge (Auxvasse) registered the least amount of missed precipitation for R(Z,ZDR) (101.1 mm) and R(ZDR,KDP) (105.1 mm). Overall, the R(Z,ZDR) algorithm registered the least amount of missed precipitation overall at Auxvasse.

Conversely, the R(KDP) equation was calculated to have the lowest MPA (95.6) at Williamsburg, with R(Z) and RREC both recording 98.7 mm. This accounted for 5.4 and 5.6% of the total gauge recorded rainfall amount (1769.3 mm), while R(Z,ZDR) and R(ZDR,KDP)'s MPA percentages were 9.9 and 11.3%, accordingly. Therefore, algorithms containing ZDR tend to underestimate the rain rate at

Williamsburg such that values less than 0.25 mm were registered and, ultimately, assumed no precipitation to be present. Larger magnitudes of ZDR were thus estimated by the radar, lowering the overall QPE for both R(Z,ZDR) and R(ZDR,KDP).

Due to the fact Versailles and Vandalia were 75 and 80 km from the MZZU radar, their differences in overall error were dependent upon the algorithm chosen. For example, similar to the instances when R(Z), R(KDP), and RREC were lower in MPA and the MPA percentage at Williamsburg than Auxvasse, these algorithms were more accurate at Versailles than Vandalia. This result demonstrates that the algorithms containing ZDR were superior at close (Auxvasse) and further (Vandalia) ranges from the MZZU radar, whereas the other three equations were best at intermediate distances (i.e., between 30 and 75 km).

As noted in the contingency analyses section, the number of false alarms outnumbered the counts of misses by more than six times, mirroring the number of hits, overall. Therefore, the false precipitation amount (FPA) is, unsurprisingly, approximately six times the MPA, particularly for the algorithms that did not contain ZDR. Conversely, R(Z,ZDR) and R(ZDR,KDP) recorded, approximately, twice the amount of FPA as MPA. For example, the FPA for R(Z,ZDR) at the gauge locations at increasing distances from the radar were 265.1, 295.8, 417.1, and 382.9 mm, whereas the MPA were 101.1, 175.5, 224.1, and 204.3 mm, respectively. This indicates that no MPA for R(Z,ZDR) was more than 15% of total precipitation measured at the gauge locations, whereas FPA did not exceed 27% (but was no lower than 15%). However, R(ZDR,KDP) displayed the lowest FPA, overall, at each locations such that it did not exceed 375 mm (373.1 mm at Versailles) nor did it register any less than 230 mm (233.7 mm at Auxvasse).

At all locations, the R(Z), R(KDP), and RREC overestimated the amount of total radar estimated QPE compared to the gauge recorded rainfall (Figure 7). Furthermore, the FPA tend to exceed the overall gauge recorded rainfall amount for these algorithms as well (Table 4). The only algorithm which had a lower total accumulation of radar estimated QPE than the gauge recorded amount of rainfall was

Atmos. Meas. Tech. Discuss., https://doi.org/10.5194/amt-2017-439
Manuscript under review for journal Atmos. Meas. Tech.
Discussion started: 7 December 2017

R(ZDR,KDP) at both Williamsburg and Vandalia. However, R(Z,ZDR) had more similar values (within 20 mm) at Vandalia than R(ZDR,KDP) than at Williamsburg.

The total precipitation error is the quantitative value of all errors in the QPE. In other words, it is the quantitative value of precipitation analyzed by the normalized standard error, and follows a similar pattern. The TPE for all locations analyzed by the R(KDP) equation did was not lower than 2000 mm (Table 4). Conversely, none of the ZDR-containing equations had a TPE larger than 1800 mm, but the only locations where the TPE was less than the gauge accumulated precipitation amount were at Auxvasse and Williamsburg for both R(Z,ZDR) and R(ZDR,KDP). For these two algorithms, less than 40% of the total error were due to either MPA or FPA, whereas the FPA resulted in the bulk of error for the other 3 algorithms. This indicates that most of the errors, when utilizing ZDR, were due to errors by hits.

The sum of precipitation (Figure 7) represents the amount of precipitation that would result if the direct accumulation of radar estimated QPE were conducted, such that missed precipitation were not included and false alarms were accounted for. Essentially, it acts as a long-term performance of the QPE from each algorithm at each site. From the quantitative analyses, it is seen that the ZDR-containing algorithms R(Z,ZDR) and R(ZDR,KDP) not only displayed the overall lowest MAE and NSE, but are more accurate with their overall accumulation of precipitation with respect to time (Figure 7). In other words, in spite of the relatively large FPA and MPA across all algorithms at each location, the ZDR-containing equations cancelled the FPA, MPA, and overall MAE over time, resulting in accurate gauge-accumulation precipitation amounts represented as the closeness in values to the gauge recorded rainfall and total sum of precipitation black and magenta contours in Figure 7, accordingly).

Conclusions

Atmos. Meas. Tech. Discuss., https://doi.org/10.5194/amt-2017-439
Manuscript under review for journal Atmos. Meas. Tech.
Discussion started: 7 December 2017

Atmospheric Measurement Techniques Discussions

The current study analyzed two years' worth of X-band dual-polarimetric quantitative precipitation estimates (QPE) from Central Missouri. Four separate terrestrial-based precipitation gauges (i.e., tipping buckets) served as ground-truth. Over 50 algorithms were tested, of which the analyses of the five best from each grouping of algorithms from R(Z), R(Z,ZDR), R(KDP), R(ZDR,KDP), and echo classifiers, were reported. Statistical, contingency, and overall quantitative analyses were reported to determine not only the best performing algorithms overall, but to determine the course of the error.

The best equations were determined to be the R(Z)-Convective algorithm, an NSSL-derived R(Z,ZDR) equation from Ryzhkov et al., (2003, 2005), an R(KDP) equation from Matrosov (2010), an R(ZDR,KDP) equation from Koffi et al. (2014), and the rain rate echo classifier. Algorithms containing reflectivity typically exhibited negative biases, of which, the R(Z,ZDR) had the lowest bias values, overall. Conversely, the KDP-containing algorithms showed positive biases, with the R(KDP) being the largest, overall.

Overall, the R(Z,ZDR) and R(ZDR,KDP) equations performed the best. This was evidenced as these algorithms having the lowest MAE and NSE at nearly every gauge location. Furthermore, these were the only equations which exhibited NSE values below 100 %, particularly at the two closest gauge locations (30 and 45 km from the radar). However, these equations had the overall lowest correlation coefficient (R^2) values in comparison to the other algorithms. It is theorized that these low R^2 values were due, primarily, from an overall larger spread in the QPE's from these particular equations. The R(Z), R(KDP), and RREC algorithms exhibited correlation values as large as 0.70 at the closest gauge location, while values as low as 0.5 were reported at the furthest location (Vandalia, 80 km). A typical reduction in R^2 values were observed as range from the radar increased.

The majority of the error from the QPE's at each location were due to false alarms, potentially due to evaporation (Kumjian and Ryzhkov, 2010; Martinaitis et al., 2017). In some instances, particularly for R(Z), R(KDP), and RREC, the false precipitation amounts were up to 65% of the total of the gauge accumulated rainfall amounts. Conversely, the ZDR-containing equations displayed not only the lowest missed and false precipitation amounts, but the overall accumulation of precipitation from these two equations were most similar to the accumulated gauge rainfall amounts, thus indicating the robust performance of the utilization of ZDR in QPE estimates.

The results presented display the accuracy of X-band QPE estimates. It is noted that, however, no equations were derived and tested for the current study. The results of the performance of the radar may be improved by not only comparing results to disdrometer data, but also from combinations of the algorithms at specific rain rates, much like the overall Joint Polarization (Ryzhkov et al., 2005; Giangrande and Ryzhkov 2008) and CSU-CHILL (Cifelli et al., 2011) algorithms. The promising results, particularly through the implementation of the differential reflectivity, further the considerations as to installing the devices as permanent, cost-effective solutions to the WSR-88D NEXRAD system, especially in regions where a gap in the radar coverage exists.

Acknowledgements

This material is based upon work supported by the National Science Foundation under Award Number IIA-1355406. Any opinions, findings, and conclusions or recommendations expressed in this material are those of the authors and do not necessarily reflect the views of the National Science Foundation.

Literature cited

Alaya, M.A., Ourda, T.B.M.J., and Chebana, F., 2017: Non-Gaussian spatiotemporal simulation of multisite precipitation: Downscaling framework. *Climate Dyn.* doi: https://doi.org/10.1007/s00382-017-3578-0.

Anognostou, E.N., Anognostou M.N, Krajewski W.F., Kruger A., and Mirovsky, B.J., 2004: High resolution rainfall estimation from X-band polarimetric radar measurements. *J. Hydrometeor.*, **5**, 110-128.

Atlas, D., 2002: Radar calibration: Some simple approaches. *Bull. Am. Meteorol. Soc.*, **83**, 1313-1316.

Berne, A., and Krajewski, W.F., 2013: Radar for hydrology: Unfulfilled promise or unrecognized potential? *Adv. Water Resour.*, **51**, 357-366.

Brandes, E.A., Zhang, G., and Vivekanandan, J., 2002: Experiments in rainfall estimation with a polarimetric radar in a subtropical environment. *J. Appl. Meteor. Climatol.*, **41**, 674-685.

Bringi, V.N., and Chandrasekar, V., 2001: Polarimetric Doppler weather radar, principles and applications. Cambridge University Press: Cambridge, UK; 636.

Chai, T., and Draxler, R.R., 2014: Root mean square error (RMSE) or mean absolute error (MAE)? – Arguments against avoiding RMSE in the literature. *Geosci. Model Dev.*, **7**, 1247-1250.

Ciach, G.J., and Krajewski, W.F., 1999a: Radar-raingage comparisons under observational uncertainties. *J. Appl. Meteorol.*, **38**, 1519-1525.

Ciach, G.J., and Krajewski, W.F., 1999b: On the estimation of radar rainfall error variance. *Adv. Water Resour.*, **22**, 585-595.

Ciach, G.J., 2002: Local Random Errors in Tipping-Bucket Rain Gauge Measurements. *J. Atmos. Oceanic Technol.*, **20**, 752-759.

Cifelli, R., Chandrasekar, V., Lim, S., Kennedy, P.C., Wang, Y., and Rutledge, S.A., 2011: A new dual-polarization radar rainfall algorithm: Application in Colorado precipitation events. *J. Atmos. Oceanic Tech.*, **28**, 352-364.

Cunha, L.K., Smith, J.A., Baeck, M.L., and Krajewski, W.F., 2013: An early performance of the NEXRAD dual-polarization radar rainfall estimates for urban flood applications. *Wea. Forecasting*, **28**, 1478-1497.

Fabry, F., Bellon, A., Duncan, M.R., and Austin, G.L., 1994: High resolution rainfall measurements by radar for very small basins: the sampling problem reexamined. *J. Hydrol.*, **161**, 415-428.

Fairman, J.G., Schultz, D.M., Kirschbaum, D.J., Gray, S.L., and Barrett, A.I., 2012: A radar-based rainfall climatology of Great Britain and Ireland. *Weather*, **70**, 153-158.

Giangrande, S.E., and Ryzhkov, A.V., 2008: Estimation of rainfall based on the results of polarimetric echo classification. *J. Appl. Meteor. Climatol.*, **47**, 2445-2462.

Gorgucci, E., Scarchilli, G., and Chandrasekar, V., 1999: Specific differential phase estimation in the presence of nonuniform rainfall medium along the path. *J. Atmos. Oceanic Technol.*, **16**, 1690-1697.

Goudenhoofdt, E., and Delobbe, L, 2012: Long-term evaluation of radar QPE using VPR correction and radar-gauge merging. *Intl. Assoc. Hydrol. Sci. Pub.*, **351**, 249-254.

Goudenhoofdt, E., and Delobbe, L., 2016: Generation and verification of rainfall estimates from 10-yr volumetric weather radar measurements. *J. Hydrol.*, **133**, 1191-1204.

Atmos. Meas. Tech. Discuss., https://doi.org/10.5194/amt-2017-439
Manuscript under review for journal Atmos. Meas. Tech.
Discussion started: 7 December 2017

Atmospheric Measurement Techniques Discussions

Gourley, J.J., Giangrande, S.E., Hong, Y., Flamig. Z,, Schuur, T., and Vrugt, J., 2010: Impacts of polarimetric radar observations on hydrologic simulation. *J. Hydrometeorol.*, **11**: 781-796.

Habib, E., Krajewski, W.F., Nespor, V., and Kruger, A., 1999: Numerical simulation studies of rain gauge data correction due to wind effect. *J. Geophys. Res.*, **104**, 723–734.

Habib, E., Krajewski, W.F., and Kruger, A., 2001: Sampling errors of tipping-bucket rain gauge measurements. *J. Hydrol. Eng.*, **6**, 159-166.

Haylock, M.R., Hofstra, N., Klein Tank, A.M.G., Klok, E.J., Jones, P.D., and New, M., 2008: A European daily high-resolution gridded data set of surface temperature and precipitation for 1950-2006. *J. Geophys. Res.*, **113**. doi: https://doi.org/10.1029/2008JD010201.

Hubbert, J., and Bringi, V.N., 1995: An iterative filtering technique for the analysis of copular differential phase and dual-frequency polarimetric variables. *J. Atmos. Oceanic. Technol.*, **12**, 643-648.

Ice, R.L., Heck, A.K., and Cunningham, J.G., 2013: Polarimetric weather radar calibration – engineering challenges. *36th Conf. on Radar Meteorology, Albuquerque, NM, Amer. Meteor. Soc.*

Jerez, S., Pedro Montavez, J., Jimenez-Guerrero, P., Jose Gomez-Navarro, J., Lorente-Plazas, R., and Zorita, E., 2013: A multi-physics ensemble of present-day climate regional simulations over the Iberia Peninsula. *Clim. Dynam.*, **40**, 3023-3046.

Illingworth, A., 2004: Improved precipitation rates and data quality by using polarimetric measurements. *Weather Radar: Principles and Advanced Applications*. Springer, 130-166.

Kitchen, M. and Jackson, P.M., 1993: Weather radar performance at long range – simulated and observed. *J. Appl. Meteor.*, **32**, 975-985.

Kumjian, M.R., and Ryzhkov, A.V., 2010: The impact of evaporation on polarimetric characteristics of rain: Theoretical model and practical applications. *J. Appl. Meteor. Climatol.*, **49**, 1247-1267.

Klazura, G.E., and Kelly, D.S., 1995: A comparison of high resolution rainfall accumulation estimates from the WSR-88D precipitation algorithm with rain gage data. Preprints, *27th Conf. on Radar Meteor.*, Vail, CO., Amer. Meteor. Soc., 31-34.

Kleiber, W., Katz, R.W., and Rajagopalan, B., 2012: Daily spatiotemporal precipitation simulation using latent and transformed Gaussian processes. *Water Res. Res.*, **48**, doi: https://doi.org/10.1029/2011WR011105.

Koffi, A.K., Gosset, M., Zahiri, E.P., Ochou, A.D., Kacou, M., Cazenave, F., and Assamoi, P., 2014: Evaluation of X-band polarimetric radar estimation of rainfall and rain drop size distribution parameters in West Africa. *Atmos. Res.*, **143**, 438-461.

Lakshmanan, V., Smith, T., Stumpf, G., and Hondl, K., 2007a: The warning decision support system—integrated information. *Wea. Forecasting*, **22**, 596–612.

Lakshmanan, V., Fritz, A., Smith, T., Hondl, K., and Stumpf, G., 2007b: An automated technique to quality control radar reflectivity data. *J. Appl. Meteor. Climatol.*, **46**, 288-305.

Lakshmanan, V., Zhang, J., and Howard, K., 2010: A technique to censor biological echoes in radar reflectivity data. *J. Appl. Meteor. Climatol.*, **49**, 453-462.

Lakshmanan, V., Karstens, C., Kruse, J., and Tang, L, 2014: Quality control of weather radar data using polarimetric variables. *J. Atmos. Oceanic Tech.*, **31**, 1234-1249.

Martinaitis, S.M., Grams, H.M., Langston, C., Zhang, J., and Howard, K., 2017: A real-time evaporation correction scheme for radar-derived mosaicked precipitation estimations. Doi:10.1175/JHM-D-17-0093.1, in press.

Matrosov, S.Y., Clark, K.A., Martner, B.E., and Tokay, A., 2002: X-band polarimetric radar measurements of rainfall. *J. Appl. Meteor.*, **41**, 941-952.

Matrosov, S.Y, 2010: Evaluating polarimetric X-band radar rainfall estimators during HMT. *J. Atmos. Oceanic Technol.*, **27**, 122-134.

McLaughlin, D., Pepyne, D., Chandrasekar, V., Phillips, B., Kurose, J., Zink, M., Droegemeier, K., Cruz-Pol, S., Junyent, F., Brotzge, J., Westbrook, D., Bharadwaj, N., Wang, Y., Lyons, E., Hondl, K., Liu, Y., Knapp, E., Xue, M., Hopf, A., Kloesel, K., Defonzo, A., Kollias, P., Brewster, K., Contreras, R., Dolan, B., Djaferis, T., Insanic, E., Frasier, S., and Carr, F., 2009: Short-wavelength technology and the potential for distributed networks of small radar systems. *Bull. Amer. Meteor. Soc.*, **90**, 1797-1817.

Ogden, F.L., Sharid, H.O., Senarath, S.U.S., Smith, J.A., Baeck, M.L., and Richardson, J.R., 2000: Hydrologic analysis of the Fort Collins, Colorado, flash floods of 1997. *J. Hydrol.*, **228**: 82-100.

Park, S.G., Maki, M., Iwanami, K., Bringi, V.N., and Chandrasekar, V., 2005: Correction of radar reflectivity and differential reflectivity for rain attenuation at X band. Part II: Evaluation and application. *J. Atmos. Oceanic Technol.*, **22**, 1633-1655.

Rasmussen, R., Baker, B., Kochendorfer, J., Meyers, T., Landolt, S., Fischer, A.P., Black, J., Theriault, J.M., Kucera, P., Gochis, D., Smith, C., Nitu, R., Hall, M., Ikeda, K., and Gutmann, E., 2012: How well are we measuring snow: The NOAA/FAA/NCAR winter precipitation test bed. *Bull. Amer. Meteor. Soc.*, **93**, 811-829.

Ryzhkov, A.V., Giangrande, S., and Schurr, T., 2003: Rainfall measurements with the polarimetric WSR-88D radar. National Severe Storms Laboratory Rep. Norman: OK, 98 pg.

Ryzhkov, A.V., Giangrande, S., and Schurr, T., 2005: Rainfall estimation with a polarimetric prototype of WSR-88D. *J. Appl. Meteor.*, **44**, 502–515.

Seo, B.-C., Dolan, B., Krajewski, W., Rutledge, S.A., and Petersen, W., 2015: Comparison of single- and dual-polarization-based rainfall estimates using NEXRAD data for the NASA Iowa flood studies project. *J. Hydrometeor.*, **16**, 1658-1675.

Sevruk, B., 2005: Rainfall measurement: Gauges. *Enc. Hydrol. Sci.*, M.G. Anderson, Ed., John Wiley & Sons Ltd., 529-536.

Shucksmith, P.E., Sutherland-Stacey, L., and Augstin, G.L., 2011: The spatial and temporal sampling errors inherent in low resolution radar estimates of rainfall. *Meteorol. App.*, **18**, 354-360.

Simpson, M.J., Hubbart, J.A., and Fox, N.I., 2016: Ground truthed performance of single and dual-polarized radar rain rates at large ranges. *Hydrol. Process.*, **30**, 3692-3703.

Smith, J.A., Seo, D.J., Baeck, M.L., and Hudlow, M.D., 1996: An intercomparison study of NEXRAD precipitation estimates. *Water Resour. Res.*, **32**, 2035-2045.

Vieux, B.E., 2004. Distributed hydrologic modeling using GIS, 2nd ed. Water Science Technology Series. Vol. 48. Kluwer Academic Publishers, Norwell, Massachusetts. ISBN 1-4020-2459-2.

Vieux, B.E., and Bedient, P.B., 2004: Hydrologic prediction accuracy assessment using radar rainfall. *World Water Congress*, **138**, 273.

Vieux, B.E., Cui, Z., and Guar, A., 2004: Evaluation of a physics-based distributed hydrologic model for flood forecasting. *J. Hydrol.*, **298**, 155-177.

Vieux, B.E., and Imgarten, J.M., 2012: On the scale-dependent propagation of hydrologic uncertainty using high-resolution X-band radar rainfall estimates. *Atmos. Res.*, **103**, 96-105.

Wang, Y., and Chandrasekar, V., 2010. Quantitative precipitation estimation in the CASA X-band dual-polarization radar network. *J. Atmos. Oceanic Technol.*, **27**, 1665-1676.

Williams, C.R., Gage, K.S., Clark, W., and Kucera, P., 2005: Monitoring the reflectivity calibration of a scanning radar using a profiling radar and a disdrometer. *J. Atmos. Oceanic Technol.*, **22**, 1004-1018.

Willmott, C., and Matsuura, K., 2005: Advantages of the Mean Absolute Error (MAE) over the Root Mean Square Error in assessing average model performance. *Clim. Res.*, **30**, 79-82.

Zrnic, D.S., and Ryzhkov, A.V., 1996: Advantages of rain measurements using specific differential phase. *J. Atmos. Oceanic Tech.*, **13**, 454-464.

Zrnic, D.S., Doviak, R., Zhang, G., and Ryzhkov, A.V., 2010: Bias in differential reflectivity due to cross coupling through the radiation patterns of polarimetric weather radars. *J. Atmos. Oceanic Technol.*, **27**, 1624-1637.

Figures

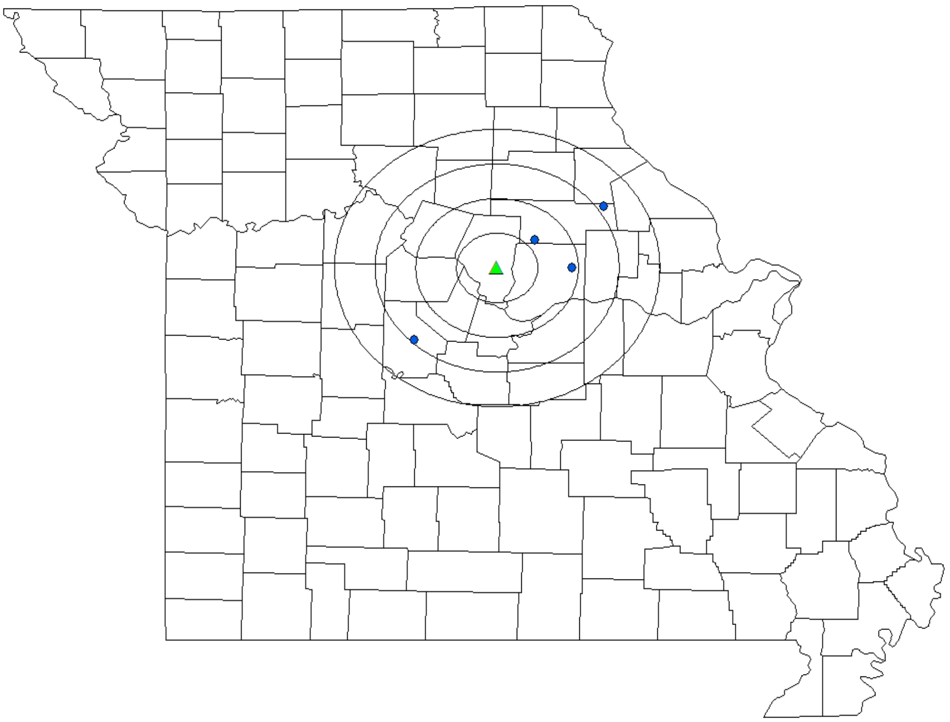

Figure 1. Study location including to the four gauges utilized for the current study. From left-to-right, the gauges are Versailles, Auxvasse, Williamsburg, and Vandalia, MO. The MZZU X-band radar is plotted in addition to 25-, 50-, 75-, and 100-km range rings.

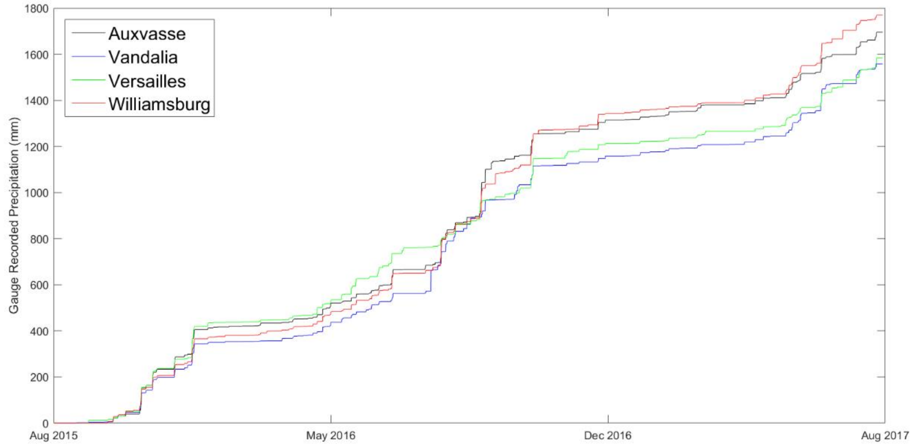

Figure 2. Accumulated gauge-recorded precipitation from the beginning to the end of the study for the four-separate terrestrial-based tipping buckets.

Atmos. Meas. Tech. Discuss., https://doi.org/10.5194/amt-2017-439
Manuscript under review for journal Atmos. Meas. Tech.
Discussion started: 7 December 2017

Atmospheric Measurement Techniques
Discussions
Open Access

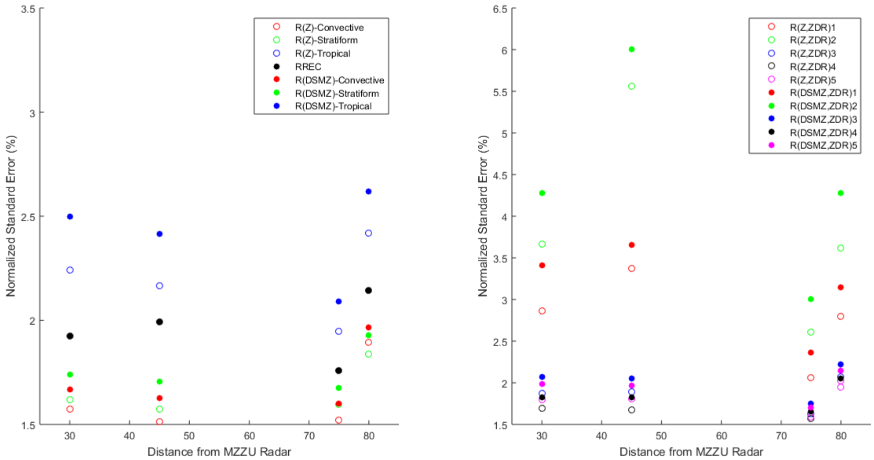

Figure 3. Performance of the 3 R(Z) and 3 R(DSMZ), RREC, 5 R(Z,ZDR) and 5 R(DSMZ,ZDR) S-band equations at each of the four gauge locations.

Atmos. Meas. Tech. Discuss., https://doi.org/10.5194/amt-2017-439
Manuscript under review for journal Atmos. Meas. Tech.
Discussion started: 7 December 2017

Atmospheric Measurement Techniques
Discussions

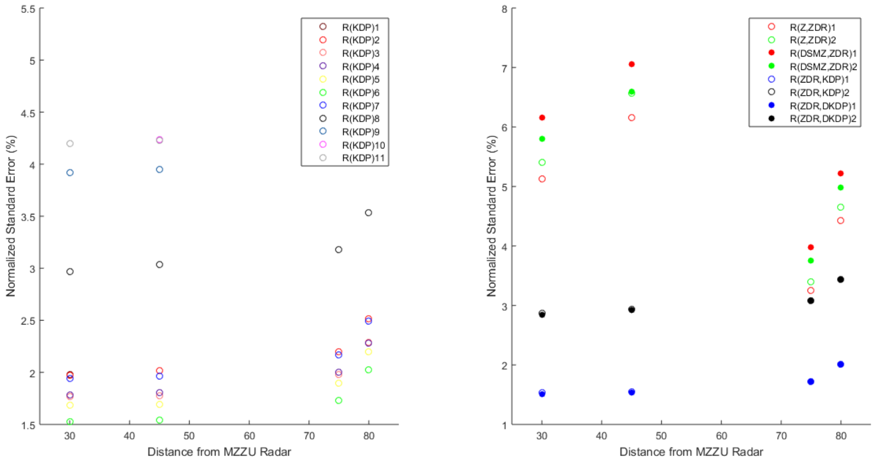

Figure 4. Performance of the 11 R(KDP), 2 R(Z,ZDR), 2 R(DSMZ,ZDR), 2 R(ZDR,KDP), and 2 R(ZDR,DKDP) X-band algorithms at each of the four gauge locations.

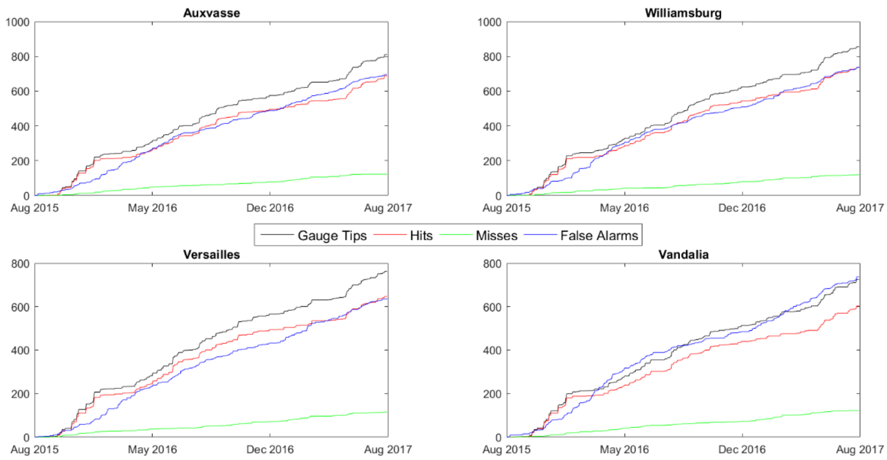

Figure 5. Contingency analyses at each of the four gauges utilized for the current study utilizing the R(ZDR,KDP) equation, including the accumulated number of tipping bucket tips, hits, misses, and false alarms.

Atmos. Meas. Tech. Discuss., https://doi.org/10.5194/amt-2017-439
Manuscript under review for journal Atmos. Meas. Tech.
Discussion started: 7 December 2017

Atmospheric Measurement Techniques
Discussions

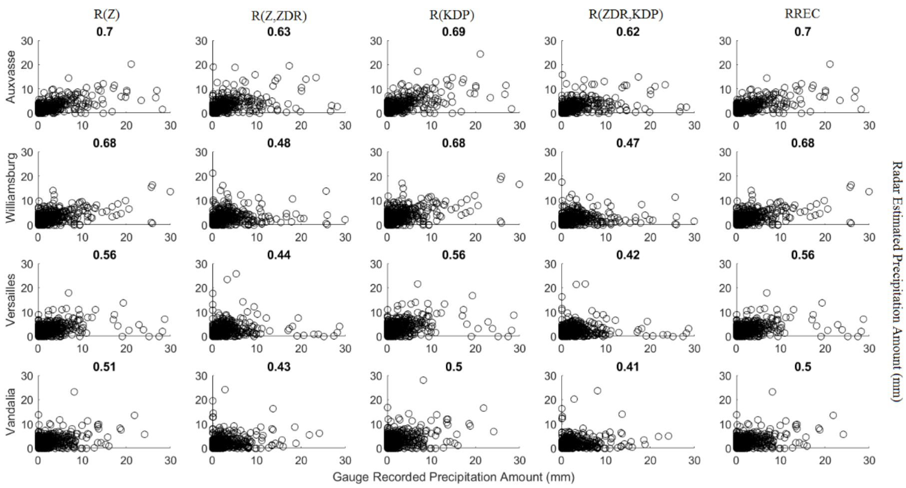

Figure 6. Correlation coefficient values based on the comparison of the gauge recorded (abscissa) and radar estimated (ordinate) rainfall amounts for each of the five-best performing algorithms at each of the four gauges utilized.

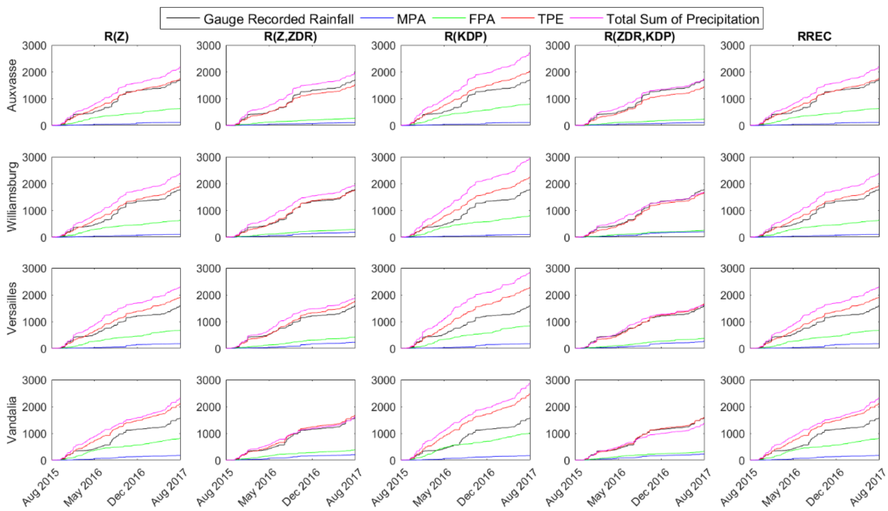

Figure 7. Cumulative sum of the gauge recorded precipitation, missed precipitation amount (MPA), false precipitation amount (FPA), total precipitation error (TPE), and the overall accumulation of precipitation estimated by the specified radar QPE algorithm at each of the four gauges locations.

Tables

Table 1. MZZU X-band radar characteristics.

Variable	Value
Location (x,y)	38.906°N, -92.269°W
Altitude Above Ground Level	308 m
Dual Pulse Repetition Frequency	5:4 Stagger: 2,000 Hz – 124 kts
Radar Type	EWR Solid State: Parabolic prime focus composite reflector (Dish mounted radome cover)
Peak Power	1 kW standard
Frequency	9.35 GHz ± 50 MHz (User Selectable)
Pulse Width	1 – 80 μs
Diameter	1.82 m
Beamwidth	1.27°
Gain	42 dB
Sensitivity	(80 μs at 50 km range): -1.5 dBZ
Elevation Angle	-5° to 120°

Table 2. List of X-band polarimetric algorithms used for radar rainfall estimates.

$R(KDP) = aKDP^{b}$				
Algorithm number	a	b	c	References
1	17.0	0.73	-	Matrosov (2010)
2	16.5	0.71	-	Matrosov (2010)
3	16.6	0.82	-	Matrosov (2010)
4	14.4	0.71	-	Matrosov (2010)
5	16.4	0.80	-	Matrosov (2010)
6	14.9	0.79	-	Matrosov (2010)
7	47.3	0.79	-	WC (2010)
8	18.2	0.79	-	WC (2010)
9	19.6	0.82	-	WC (2010)
10	13.6	0.83	-	Koffi et al. (2014)
11	21.0	0.57	-	Koffi et al. (2014)
$R(Z, ZDR) = aZ^{b}ZDR^{c}$				
Algorithm number				References
1	0.0039	1.07	-5.97	Matrosov (2010)
2	0.0056	1.02	-5.60	Matrosov (2010)
$R(ZDR, KDP) = aZDR^{b}KDP^{c}$				
Algorithm number				References
1	15.1	-0.29	0.94	Koffi et al. (2014)
2	20.9	-0.05	0.59	Koffi et al. (2014)

Atmos. Meas. Tech. Discuss., https://doi.org/10.5194/amt-2017-439
Manuscript under review for journal Atmos. Meas. Tech.
Discussion started: 7 December 2017

Atmospheric Measurement Techniques Discussions

Table 3. Statistical analyses for the MZZU radar and the best algorithms from each grouping of equations with their respective distance from the radar.

Algorithm	**Auxvasse 30 km**	**Williamsburg 45 km**	**Versailles 75 km**	**Vandalia 80 km**
R(Z)	Bias: -0.1 MAE: 1.3 NSE: 102.6	Bias: -0.3 MAE: 1.4 NSE: 107.8	Bias: -0.2 MAE: 1.4 NSE: 119.9	Bias: -0.4 MAE: 1.5 NSE: 134.6
R(Z,ZDR)	Bias: 0.0 MAE: 1.3 NSE: 89.2	Bias: -0.2 MAE: 1.6 NSE: 99.0	Bias: -0.3 MAE: 1.6 NSE: 110.5	Bias: -0.2 MAE: 1.5 NSE: 106.9
R(KDP)	Bias: 0.3 MAE: 1.3 NSE: 119.1	Bias: 0.4 MAE: 1.3 NSE: 126.1	Bias: 0.5 MAE: 1.5 NSE: 142.5	Bias: 0.6 MAE: 1.6 NSE: 158.6
R(ZDR,KDP)	Bias: 0.3 MAE: 1.2 NSE: 84.7	Bias: 0.3 MAE: 1.3 NSE: 93.1	Bias: 0.5 MAE: 1.4 NSE: 104.7	Bias: 0.5 MAE: 1.5 NSE: 101.8
RREC	Bias: 0.5 MAE: 1.6 NSE: 103.1	Bias: 0.2 MAE: 1.7 NSE: 108.1	Bias: 0.2 MAE: 1.7 NSE: 120.0	Bias: 0.1 MAE: 1.7 NSE: 135.1

Table 4. Quantitative analyses, including the missed precipitation amount (MPA), false precipitation amount (FPA), and total precipitation error (TPE). Percent indicates the relative error due to either MPA or FPA relative to the gauge accumulated precipitation amount (Gauge Precip row).

	Auxvasse	Williamsburg	Versailles	Vandalia
Gauge Precip	1695.7	1769.3	1583.7	1557.4
R(Z)	MPA: 110.3 Percent: 6.5 FPA: 634.0 Percent: 37.4 TPE: 1739.6	MPA: 99.4 Percent: 5.6 FPA: 633.9 Percent: 35.8 TPE: 1906.7	MPA: 174.4 Percent: 11.0 FPA: 674.23 Percent: 42.6 TPE: 1899.3	MPA: 180.8 Percent: 11.6 FPA: 811.3 Percent: 52.1 TPE: 2096.9
R(Z,ZDR)	MPA: 101.1 Percent: 6.0 FPA: 265.1 Percent: 15.6 TPE: 1512.0	MPA: 175.5 Percent: 9.9 FPA: 295.8 Percent: 16.7 TPE: 1751.0	MPA: 224.1 Percent: 14.2 FPA: 417.1 Percent: 26.3 TPE: 1750.2	MPA: 204.3 Percent: 13.1 FPA: 382.9 Percent: 24.6 TPE: 1664.3
R(KDP)	MPA: 107.6 Percent: 6.3 FPA: 794.7 Percent: 46.9 TPE: 2020.3	MPA: 95.6 Percent: 5.4 FPA: 797.7 Percent: 45.1 TPE: 2230.6	MPA: 172.1 Percent: 10.9 FPA: 840.6 Percent: 53.1 TPE: 2256.6	MPA: 171.9 Percent: 11.0 FPA: 1012.1 Percent: 65.0 TPE: 2470.4
R(ZDR,KDP)	MPA: 105.1 Percent: 6.2 FPA: 233.7 Percent: 13.8 TPE: 1436.5	MPA: 200.4 Percent: 11.3 FPA: 254.2 Percent: 14.4 TPE: 1647.1	MPA: 268.8 Percent: 17.0 FPA: 373.1 Percent: 23.6 TPE: 1657.3	MPA: 224.4 Percent: 14.4 FPA: 321.8 Percent: 20.7 TPE: 1586.0
RREC	MPA: 109.3 Percent: 6.4	MPA: 98.7 Percent: 5.6	MPA: 174.2 Percent: 11.0	MPA: 180.8 Percent: 11.6

	FPA: 635.2 Percent: 37.5 TPE: 1748.0	FPA: 635.2 Percent: 35.9 TPE: 1912.7	FPA: 674.2 Percent: 42.6 TPE: 1899.9	FPA: 811.3 Percent: 52.1 TPE: 2103.6